Formation of the –N(NO)N(NO)– polymer at high pressure and stabilization at ambient conditions

Hai Xiao, Qi An, William A. Goddard III[1], Wei-Guang Liu, and Sergey V. Zybin

Materials and Process Simulation Center, California Institute of Technology, Pasadena, CA 91125

A number of exotic structures have been formed through high-pressure chemistry, but applications have been hindered by difficulties in recovering the high-pressure phase to ambient conditions (i.e., one atmosphere and 300 K). Here we use dispersion-corrected density functional theory [PBE-*ulg* (Perdew-Burke-Ernzerhof flavor of DFT with the universal low gradient correction for long range London dispersion)] to predict that above 60 gigapascal (GPa) the most stable form of N_2O (the laughing gas in its molecular form) is a one-dimensional polymer with an all-nitrogen backbone analogous to *cis*-polyacetylene in which alternate N are bonded (ionic covalent) to O. The analogous *trans*-polymer is only 0.03~0.10 eV/molecular unit less stable. Upon relaxation to ambient conditions, both polymers relax below 14 GPa to the same stable nonplanar *trans*-polymer. The predicted phonon spectrum and dissociation kinetics validates the stability of this *trans*-poly-NNO at ambient conditions, which has potential applications as a type of conducting nonlinear optical polymer with all-nitrogen chains and as a high-energy oxidizer for rocket propulsion. This work illustrates *in silico* materials discovery particularly in the realm of extreme conditions (very high pressure or temperature).

DFT | high pressure physics and chemistry | prediction of novel materials

With strong interplay between experiment and theory, such molecular crystals as N_2 (1, 2), CO_2 (3, 4), CO (5, 6), NH_3 (7), and benzene (8) have been transformed into extended solids (covalent and ionic bonded networks) under high pressures. These studies have enhanced our understanding of chemical bonds under compression and provide opportunities to seek additional novel materials; however, it has been difficult to retain these remarkable structures at the ambient conditions needed for most applications (9). For CO_2, a 3D covalent network was synthesized (3) at high pressure (40 GPa) and temperature (1,800 K) that is isomorphic to the β-cristobalite phase of SiO_2 (10), with each carbon atom bonded tetrahedrally to four oxygen atoms. This phase of CO_2 was proposed to have potential applications as superhard (initial experiments estimated a bulk modulus of 365 GPa (11), but theory and experiment later found it to be 136 GPa (10, 12)), nonlinear optical, and high-energy density material, so efforts were made to quench this phase down to 1 atm and 300 K (3); however, it reverts back to the molecular phase at pressures lower than 1 GPa.

Because it is isoelectronic to CO_2 but polar, attempts were made to form an extended solid from N_2O using compression (above 20 GPa) and laser heating (above 1,000 K) in a diamond anvil (13). However, instead it decomposed into a mixture of an ionic crystal $NO^+NO_3^-$ and compressed N_2 molecules. No covalent extended framework similar to the polymeric CO_2 phase was found. Indeed, because the nitrogen atom forms one less covalent bond than the carbon atom, it is not obvious that it would be possible to construct a dense extended solid phase of N_2O other than the ionic form. Even so, we decided to use first principle method to explore a large number of space groups and bonding patterns at high pressures.

Because we start with molecular crystals of nitrous oxide (NNO) in which London dispersion attractions (van der Waals attraction) is dominant, we used the PBE-*ulg* flavor of density functional theory (DFT-*ulg*) in which corrections accounting for London dispersion attractions are included (14). We searched for high-pressure structures with two independent strategies.

In the first approach, we started with 41 known AB_2-type crystal structures, replaced A with O and B with N, and used DFT to determine the optimum atom positions and packings using a fixed density of 3.915 gm/cm^3 (a relative compression of 0.384 and the same as polymeric CO_2 at 41 GPa) (10). Then we took the new configurations from the lowest energy structures, built appropriate extended cells, and refined further with DFT to obtain the optimum stacking.

In the second approach, we used the USPEX (Universal Structure Predictor: Evolutionary Xtallography) code (15–17) based on an evolutionary algorithm developed by Romanov, Glass, and Lyakhov (15) and featuring local optimization, real-space representation, and flexible physically motivated variation operators. Here we considered a 12-atom unit cell at 40, 60, and 80 GPa.

Results

Both methods led to the same two final high-pressure structures: both corresponding to a 1D N_2O polymer but with either *cis*- (Fig. 1*B*) and *trans*- (Fig. 1*C*) conformations (*cis* is lower), predicted to be the most stable species above 60 GPa. The valence bond descriptions of these structures has an alternating N and N^+ backbone polyacetylene like zigzag chain with each N^+ forming a covalent bond to O^-. The valence bond description would suggest alternating single and double bonds (1.448 Å and 1.309 Å), which we find for *cis*; however, for *trans* we find all NN bonds to have the same bond distances (1.390 Å at 1 atm), indicating full resonance along the chain. Fig. 1 shows the enthalpies of various relevant phases of N_2O as a function of pressure, taking the ground state molecular crystal with space group $Pa\overline{3}$ (α-nitrogen structure) as the reference. For the two molecular phases, $Pa\overline{3}$ and space group $Cmca$, experiments find head-to-tail orientation disorder (18), so we considered all possible conformations in the unit cell to determine the lowest energy. The calculated dependence of crystal volume on pressure is comparable with experiment (Fig. S1), leading to a calculated transition pressure between the two molecular phases of 5.8 GPa at 0 K, compared with the experimental value of 4.8 GPa at room temperature (18).

In the range of 10–55 GPa and 1,000–3,400 K, the diamond anvil experiments on NNO observed a mixture of the ionic NO^+ NO_3^- phase in equilibrium with an N_2 molecule phase, formed from the dissociation of N_2O at high pressure and temperature (13, 19, 20). We also calculated these phases at the pressures considered here. However, the structure of $NO^+NO_3^-$ is not well-established experimentally: experiments reported the formation of monoclinic $P2_1/m$ phase ionic salt from the high-pressure
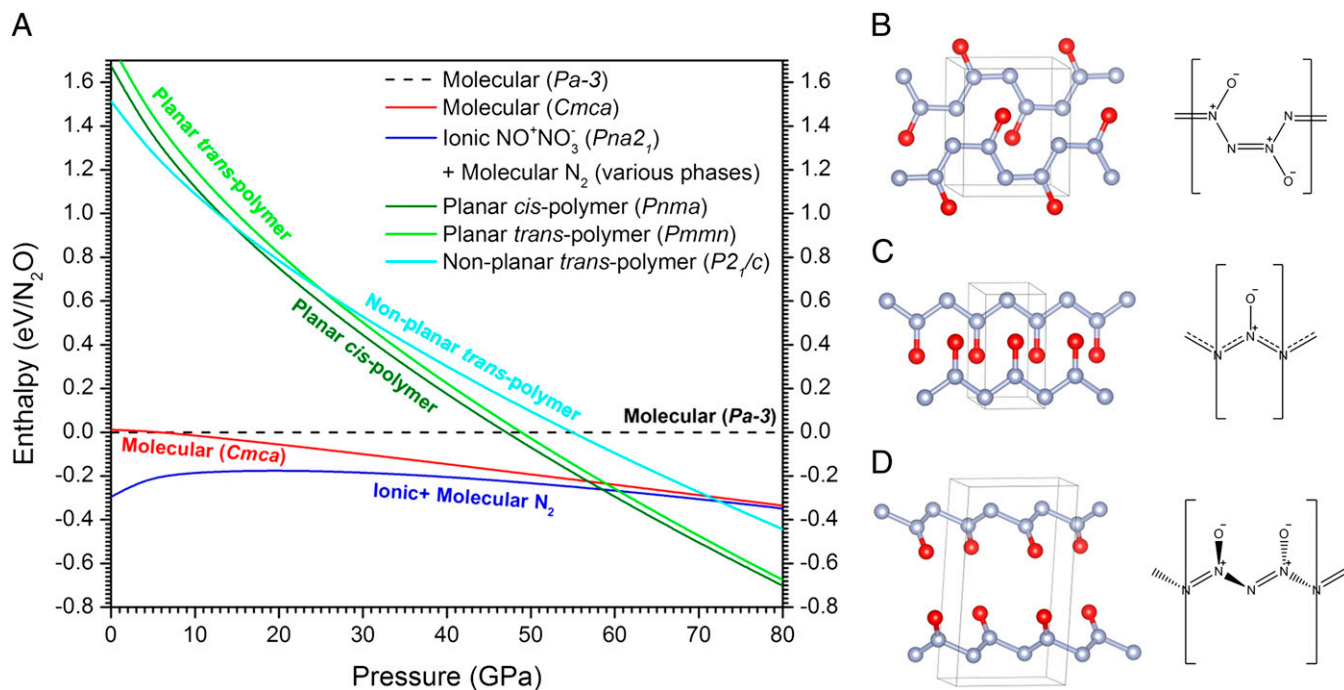

Fig. 1. (*A*) Ground state enthalpy as a function of pressure predicted for various phases of N₂O, with illustrations of crystal structures and chemical formulations of single chain for planar *cis*-polymer (*B*), planar *trans*-polymer (*C*), and nonplanar *trans*-polymer (*D*).

(2 GPa) reaction of an N_2 and O_2 mixture (21), whereas the original experiments on dissociation of N_2O under laser heating in a diamond anvil found an orthorhombic phase related to the aragonite to form after cooling (13, 22). Therefore, for the DFT study, we constructed the $NO^+NO_3^-$ crystal by cell relaxation starting with the aragonite structure. This led to an orthorhombic $Pna2_1$ phase (Fig. S2 and Table S1), which we found to be 0.03 eV per formula more stable than the monoclinic phase. We carried out DFT calculations of N_2 molecular crystals, starting with the known phases (α, γ, ε, ζ) at low temperature (23), and at each pressure, the energy calculated to be most stable was used in the enthalpy calculations. Surprisingly, this combination of $NO^+NO_3^-$ and N_2 is more stable than the NNO molecular phases for all pressures down to 0 GPa. This is plausible, as the heat of formation of N_2O molecule is 82 kJ/mol (1 kcal = 4.18 kJ) above N_2 and O_2, which were shown to form $NO^+NO_3^-$ at 2 GPa using 10.2 keV synchrotron X-ray radiation (21).

Fig. 1 shows that the *cis* and *trans* 1D polymeric phases remain energetically close (*cis* more stable by 0.03~0.10 eV/molecular unit) and become more stable than both the molecular and the mixed ionic phases at pressures above 60 GPa. Including zero point energy (ZPE) and entropy from phonons has little effect (Fig. S3):

- including ZPE to obtain the 0 K equation of state (EOS), we find that the critical pressure for the transition from the mixed ionic phase to the *cis*-polymer increases from 58.5 GPa to 61 GPa,
- while introducing entropy and enthalpy corrections to 300 K leads to a further increase to 62 GPa at 300 K (64 GPa at 500 K).

The dominant factor in determining the enthalpy at high pressure is the compressibility. For the mixed phase, the ionic $NO^+NO_3^-$ component is a dense solid, but the global compressibility of the mixed phase is dominated by the molecular phase of N_2, which polymerizes only above 110 GPa (2). In contrast, the two new NNO polymeric phases each forms a pure extended solid with mixed covalent and ionic frameworks. Thus, these phases dominate at high

pressures (where the PV term in the enthalpy becomes dominant) over all of the other phases of N_2O containing molecular forms.

The major difference between these *cis* and *trans* forms is that the planar *cis*-NNO polymer possesses alternating single and double bonds as in polyenes (polyacetylene) with an even number of carbons, whereas the planar *trans*-conformation of NNO has equal NN bond lengths (strong resonance) along the chain, perhaps due to strong electrostatic repulsion between adjacent negatively charged oxygen atoms.

We further investigated the stability of the two NNO polymers by phonon analysis. Indeed, for both crystals we find no imaginary phonon modes under high pressures, as shown in the phonon spectra in Fig. 2 (at 80 GPa), which confirms their existence as stable species (local minima). However, as the pressure is released, both crystals develop imaginary phonon modes at ~14 GPa, and both relax to one single nonplanar *trans*-conformation (Dataset S1) at zero pressure, with a phonon spectrum that attests its stability. Under high pressures, the planar conformations with their higher compressibilities are more stable, but they lead to larger electrostatic repulsion between negatively charged oxygen atom and lone-pair on nitrogen in the *cis*-case and between adjacent negatively charged oxygen atoms in the *trans*-case. It is the competition between compressibility and electrostatics that leads to the transition to the nonplanar polymer at low pressure.

Discussion

Besides accommodating electrostatics, the transition between planar and nonplanar *trans*-conformations is also accompanied by an abrupt change from uniform bonding to alternating single and double bonds, as shown in Fig. 3, implying synergistic Peierls distortion, which is relevant to the electronic properties. Therefore, we calculated band gaps of all polymeric structures (optimized with PBE-*ulg* flavor of DFT) and plotted against pressures in Fig. 3. Interestingly, PBE-*ulg* predicts that both planar NNO polymers are 1D metals, with transitions to insulators below 72 GPa for *cis*-polymer and 25 GPa for *trans*-polymer, the latter with
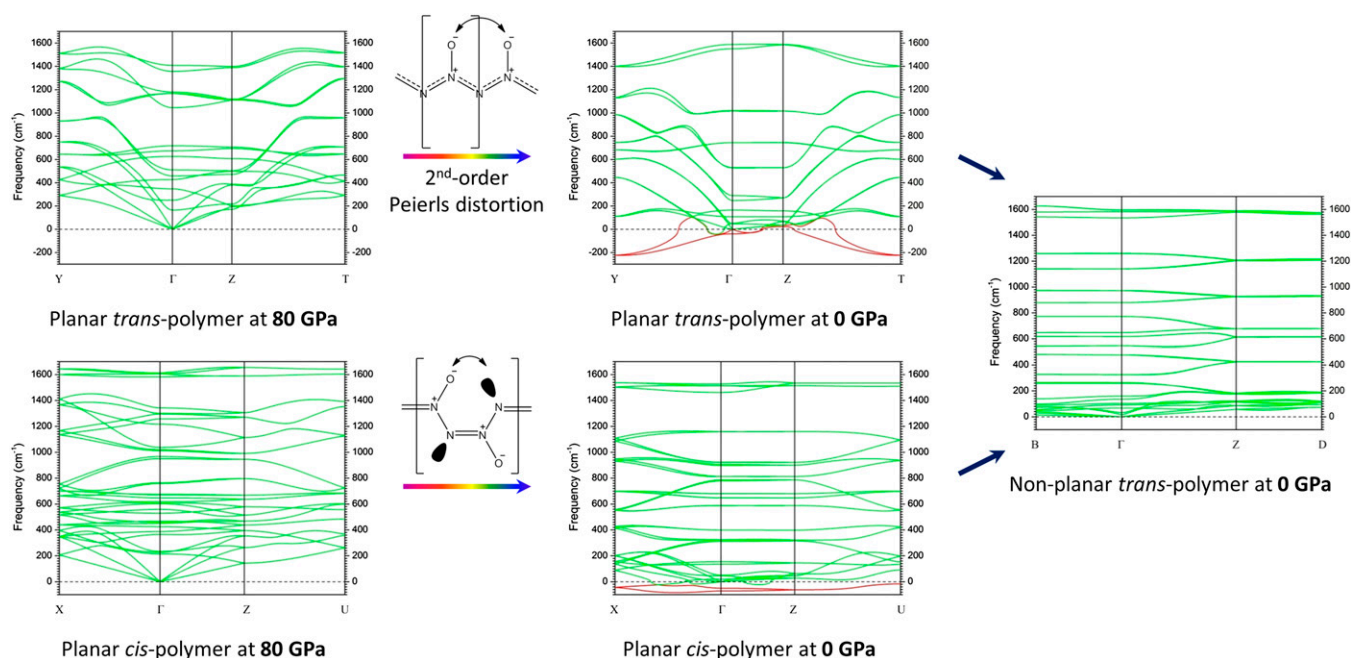
Fig. 2. Phonon spectra for polymer phases of N_2O predicted at 80 and 0 GPa. Both planar *cis*- and *trans*-polymer phases develop imaginary phonon modes, due to electrostatic repulsions and/or second-order Peierls distortion, and transform into the same nonplanar *trans*-polymer phase, the phonon spectrum of which at 0 GPa shows no imaginary modes.

simultaneous conformation transition from planar to nonplanar. Fig. 3 also shows the bond length differences between neighboring N-N bonds for the various phases. We find a trend from uniform bonding (exact for *trans*-polymer, quasi-uniform for *cis*-polymer with 0.03 Å difference) at high pressures to alternating single and double bonds when pressure is released. Combining this with the trend in band gaps indicates a first-order Peierls distortion as in polyacetylene. However, it is well documented (24, 25) that density functionals, such as PBE that are based only on local density approximation and generalized gradient approximation, significantly underestimate band gaps for insulators, due to intrinsic delocalization error (26) from including the self-interaction in the

Coulomb energy. To verify the metallic properties of these polymers under high pressures, we reinvestigated all electronic structures with the hybrid functional B3PW91 (27), which we showed to predict accurate band gaps for a wide range of semiconductors (28). In contrast to PBE, B3PW91 predicts insulating states for all three polymers throughout the whole range of pressures considered, as shown in Fig. 3. Here the density of states ([Fig. S4](#)) shows that both planar *cis*- and *trans*-polymers at high pressures with (quasi-) uniform bonding are charge-transfer insulators, with the valence band dominated by negatively charged oxygen and bridging nitrogen atoms, whereas the conduction band is dominated by the positively charged nitrogen atom. Accordingly, B3PW91 results
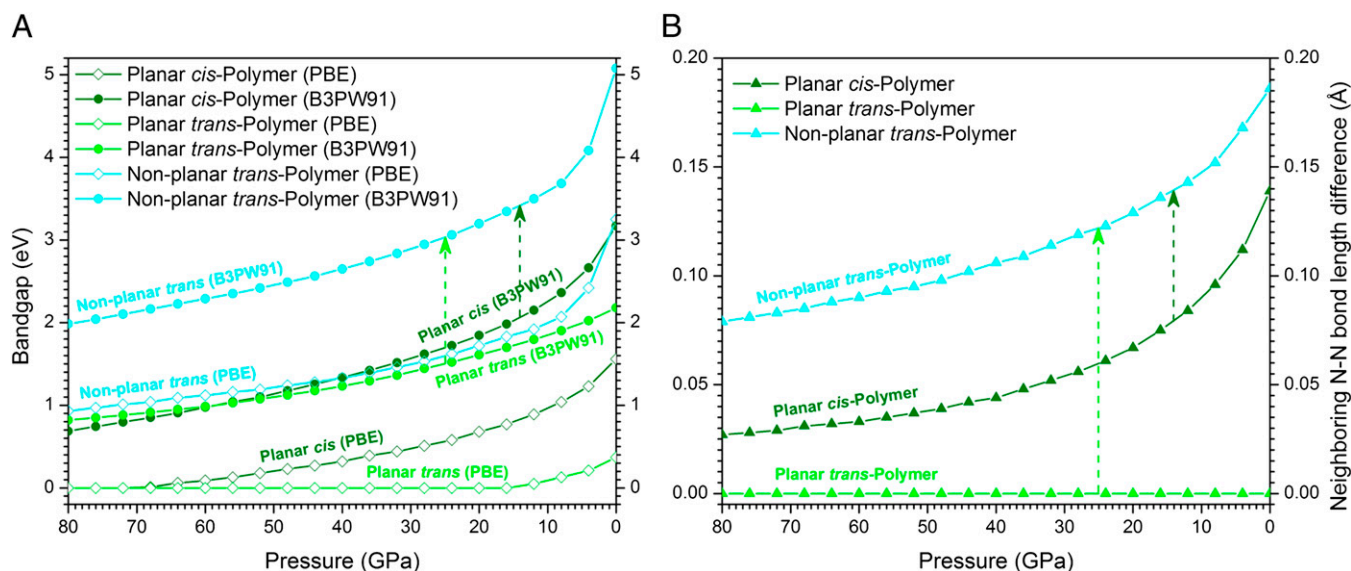
Fig. 3. Band gap (*A*) and neighboring *N*-N bond length difference (*B*) predicted as functions of pressure for all three polymer phases of N_2O at ground states. The dashed lines with arrows indicate where the transition from planar to nonplanar conformation happens.

infer the transition to be second-order Peierls distortion as in polyacene. At this point we cannot be sure whether to trust the B3PW91 or the PBE description, so it would be most valuable to carry out experiments on the conductivity or electronic spectra of these new phases.

To further evaluate the stability of nonplanar *trans*-polymer, we investigated the dissociation kinetics of the polymer, using DFT for a model oligomer containing 8 N_2O units and terminated with methyl groups at both ends. We stretched this finite chain until it fractured, locating the transition state (TS) shown in Fig. 4. This leads to an activation energy of 20.6 kcal/mol. At the TS, the partially dissociated N_2O has N-N distances of 2.062 and 1.830 Å to its two neighbors, much longer than corresponding equilibrium distances of 1.465 and 1.447 Å. This indicates that a large free space is required to activate the dissociation process, making the dissociation less favorable in the solid. This high-activation barrier of 20.6 kcal/mol from the finite model corresponds to a surface energy of 1.56×10^3 erg/cm^2, considering the packing in the crystal. Thus, we consider that it is likely that the nonplanar *trans*-polymer of N_2O will be stable at 1 atm pressure and 300 K.

After passing the TS, the oligomer would start releasing N_2O one by one from each end, accompanied with significant heat release of 40.6 kcal/mol per N_2O molecule, which might lead to catastrophic decomposition. Thus, the nonplanar *trans*-NNO polymer is a high-energy content structural material. Indeed, we calculated (PBE-*ulg*) the nonplanar N_2O *trans*-polymer to provide an internal energy release of 3.5 kJ/g when dissociated into N_2 and O_2, which is comparable to the energy release of trinitrotoluene (TNT) (4.2 kJ/g). Thus, nonplanar *trans*-NNO is a potential high-energy oxidizer for new explosive composites and rocket propellants.

Since the N_2O polymer chain is composed of alternating single and double bonds, similar to polyacetylene, albeit with an all nitrogen backbone, it might form the basis for a unique type of conducting polymer, through appropriate doping or structure modification. Similarly we expect that it might have strong nonlinear polarizabilities for nonlinear optical applications.

Summarizing, we used DFT to predict that the NNO molecular crystal can be transformed into novel polymeric phases at high pressures (beyond decomposition into mixture phase of ionic compound $NO^+NO_3^-$ and N_2 gas previously observed in experiments). The two most stable 1D N_2O polymers with planar *cis*- and *trans*-conformations were identified to be energetically favorable at pressures above 60 GPa. More importantly, when the pressure is released, these polymers transform into the same nonplanar *trans*-conformation, stable at ambient pressure and temperature. This was substantiated by analysis of the phonon spectrum and by calculating the dissociation kinetics. This unique poly-NNO material might be an excellent high-energy oxidizer for a polymer composite in which nonpolar NNO forms the matrix.

The PBE calculations suggest metallic property in the high-pressure polymer resulting from the strong resonance in these systems, which seems to disappear in the low-pressure nonplanar polymer due to changes in bonding, leading to Peierls distortion, together with electrostatic repulsions. Thus, with doping these NNO polymers, such as I, which works successfully in polyacetylene, may give rise to a new type of conducting polymer based on all-nitrogen chains. This whole work serves to illustrate the unique *in silico* process of discovering materials by theoretical modeling particularly under extreme conditions.

Methods

PBE-*ulg* calculations were performed using Vienna Ab-initio Simulation Package (VASP) package (29–31), modified to describe PBE-*ulg* and using the projector augmented wave method (32) to account for core-valence interactions. The kinetic energy cutoff for plane wave expansions was set to 500 eV, and the reciprocal space was sampled by Γ-centered Monkhorst–Pack scheme with a fine resolution of $2\pi \times 1/60$ Å^{-1}.

In the search of structures using USPEX (15–17), the kinetic energy cutoff was lowered to 400 eV, with reciprocal grids of $2\pi \times 0.06$ Å^{-1}. The convergence criteria were set to 1×10^{-6} eV energy difference for solving for the electronic wavefunction and 1×10^{-3} eV/Å force for geometry optimization.

To obtain the phonon spectra, very tight convergence criteria were used, with 1×10^{-8} eV energy difference and 1×10^{-6} eV/Å force thresholds. To calculate force constants, we used the supercell approach with finite displacements, as implemented in the Phonopy code (33).
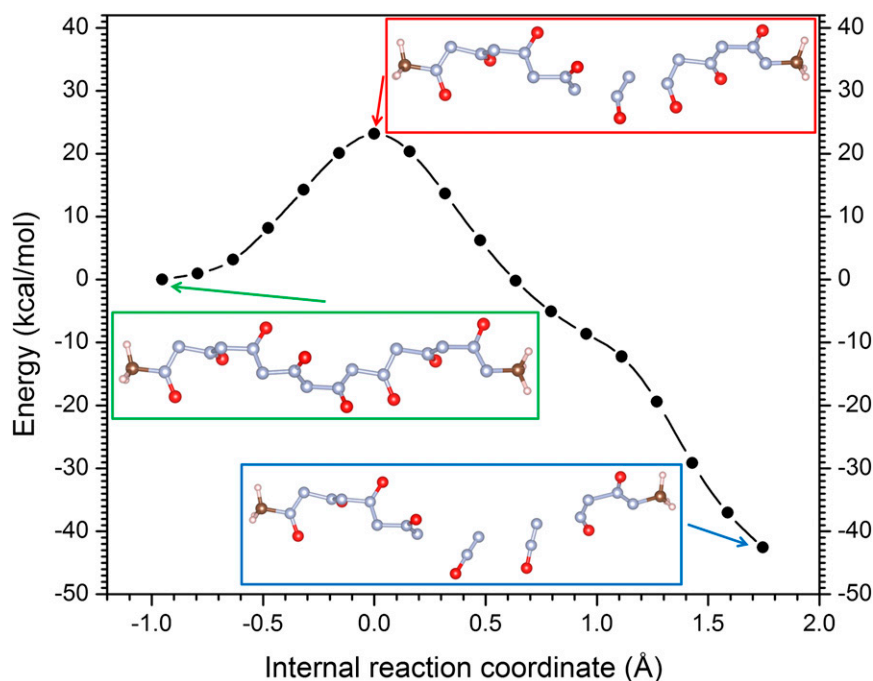

Fig. 4. Dissociation path calculated for dissociation of the model 8-mer. The oligomer contains 8 N_2O units and is terminated with methyl groups at both ends.

Xiao et al.

B3PW91 calculations were conducted using CRYSTAL09 package (34) and 6–311G* triple-zeta quality basis sets for both nitrogen and oxygen. Similar k-space grids and convergence criteria as in fine calculations with VASP were set for consistency.

For finite model calculations, the geometry optimization, Hessian calculation, and TS search were carried out at UB3LYP/6–311G*+ level using Jaguar (35). The Hessian was used to provide the vibrational frequencies for ZPE and thermo-corrections to enthalpy. The TS was shown to have exactly one imaginary vibrational mode by following the minimum energy path scan to connect reactant and product. Enthalpies are reported at 298.15 K and 1 atm.

1. Mailhiot C, Yang LH, McMahan AK (1992) Polymeric nitrogen. *Phys Rev B Condens Matter* 46(22):14419–14435.
2. Eremets MI, Gavriliuk AG, Trojan IA, Dzivenko DA, Boehler R (2004) Single-bonded cubic form of nitrogen. *Nat Mater* 3(8):558–563.
3. Iota V, Yoo CS, Cynn H (1999) Quartzlike carbon dioxide: An optically nonlinear extended solid at high pressures and temperatures. *Science* 283(5407):1510–1513.
4. Serra S, Cavazzoni C, Chiarotti GL, Scandolo S, Tosatti E (1999) Pressure-induced solid carbonates from molecular CO₂ by computer simulation. *Science* 284(5415):788–790.
5. Bernard S, Chiarotti GL, Scandolo S, Tosatti E (1998) Decomposition and polymerization of solid carbon monoxide under pressure. *Phys Rev Lett* 81(10):2092–2095.
6. Lipp MJ, Evans WJ, Baer BJ, Yoo CS (2005) High-energy-density extended CO solid. *Nat Mater* 4(3):211–215.
7. Pickard CJ, Needs RJ (2008) Highly compressed ammonia forms an ionic crystal. *Nat Mater* 7(10):775–779.
8. Ciabini L, et al. (2007) Triggering dynamics of the high-pressure benzene amorphization. *Nat Mater* 6(1):39–43.
9. McMillan PF (2002) New materials from high-pressure experiments. *Nat Mater* 1(1):19–25.
10. Datchi F, Mallick B, Salamat A, Ninet S (2012) Structure of polymeric carbon dioxide CO₂-V. *Phys Rev Lett* 108(12):125701.
11. Yoo CS, et al. (1999) Crystal structure of carbon dioxide at high pressure: "Superhard" polymeric carbon dioxide. *Phys Rev Lett* 83(26):5527–5530.
12. Dong JJ, et al. (2000) Investigation of hardness in tetrahedrally bonded nonmolecular CO₂ solids by density-functional theory. *Phys Rev B* 62(22):14685–14689.
13. Somayazulu M, et al. (2001) Novel broken symmetry phase from N₍₂₎O at high pressures and high temperatures. *Phys Rev Lett* 87(13):135504.
14. Kim H, Choi JM, Goddard WA (2012) Universal correction of density functional theory to include London dispersion (up to Lr, element 103). *J Phys Chem Lett* 3(3):360–363.
15. Oganov AR, Glass CW (2006) Crystal structure prediction using ab initio evolutionary techniques: Principles and applications. *J Chem Phys* 124(24):244704.
16. Glass CW, Oganov AR, Hansen N (2006) USPEX—Evolutionary crystal structure prediction. *Comput Phys Commun* 175(11-12):713–720.
17. Lyakhov AO, Oganov AR, Valle M (2010) How to predict very large and complex crystal structures. *Comput Phys Commun* 181(9):1623–1632.
18. Mills RL, Olinger B, Cromer DT, Lesar R (1991) Crystal-structures of N₂O to 12 GPa by X-ray-diffraction. *J Chem Phys* 95(7):5392–5398.
19. Yoo CS, et al. (2003) Disproportionation and other transformations of N₂O at high pressures and temperatures to lower energy, denser phases. *J Phys Chem B* 107(24):5922–5925.
20. Iota V, Park JH, Yoo CS (2004) Phase diagram of nitrous oxide: Analogy with carbon dioxide. *Phys Rev B* 69(6):064106.
21. Meng Y, et al. (2006) Hard x-ray radiation induced dissociation of N₂ and O₂ molecules and the formation of ionic nitrogen oxide phases under pressure. *Phys Rev B* 74(21):214107.
22. Song Y, Somayazulu M, Mao HK, Hemley RJ, Herschbach DR (2003) High-pressure structure and equation of state study of nitrosonium nitrate from synchrotron x-ray diffraction. *J Chem Phys* 118(18):8350–8356.
23. Katzke H, Toledano P (2008) Theoretical description of pressure- and temperature-induced structural phase transition mechanisms of nitrogen. *Phys Rev B* 78(6):064103.
24. Perdew JP, Levy M (1983) Physical content of the exact Kohn-Sham orbital energies: Band-gaps and derivative discontinuities. *Phys Rev Lett* 51(20):1884–1887.
25. Sham LJ, Schluter M (1983) Density-functional theory of the energy gap. *Phys Rev Lett* 51(20):1888–1891.
26. Mori-Sánchez P, Cohen AJ, Yang WT (2008) Localization and delocalization errors in density functional theory and implications for band-gap prediction. *Phys Rev Lett* 100(14):146401.
27. Becke AD (1993) Density-functional thermochemistry. III. The role of exact exchange. *J Chem Phys* 98(7):5648–5652.
28. Xiao H, Tahir-Kheli J, Goddard WA (2011) Accurate band gaps for semiconductors from density functional theory. *J Phys Chem Lett* 2(3):212–217.
29. Kresse G, Hafner J (1993) Ab initio molecular dynamics for liquid metals. *Phys Rev B Condens Matter* 47(1):558–561.
30. Kresse G, Furthmuller J (1996) Efficiency of ab-initio total energy calculations for metals and semiconductors using a plane-wave basis set. *Comput Mater Sci* 6(1):15–50.
31. Kresse G, Furthmüller J (1996) Efficient iterative schemes for ab initio total-energy calculations using a plane-wave basis set. *Phys Rev B Condens Matter* 54(16):11169–11186.
32. Kresse G, Joubert D (1999) From ultrasoft pseudopotentials to the projector augmented-wave method. *Phys Rev B* 59(3):1758–1775.
33. Togo A, Oba F, Tanaka I (2008) First-principles calculations of the ferroelastic transition between rutile-type and CaCl₂-type SiO₂ at high pressures. *Phys Rev B* 78(13):134106.
34. Dovesi R, et al. (2009) *CRYSTAL 2009 User's Manual* (Univ of Torino, Torino, Italy).
35. Schrödinger, LLC (2010) Jaguar (Schrödinger, New York), Version 7.7.

CHEMISTRY